Enhancing Epidemiological Models with Activity-Travel Behavior and Risk Perception: A Simulation Framework for Policy Management

Cloe Cortes Balcells

Rico Krueger

Michel Bierlaire

STRC conference paper 2024 **April 30, 2024**

STRC | **24th Swiss Transport Research Conference**
Monte Verità / Ascona, May 15-17, 2024

Enhancing Epidemiological Models with Activity-Travel Behavior and Risk Perception: A Simulation Framework for Policy Management

Cloe Cortes Balcells
Transport and Mobility Laboratory
Ecole Polytechnique Federale de Lausanne (EPFL)
cloe.cortesbalcells@epfl.ch

Rico Krueger
Department of Technology, Management and Economics
Technical University of Denmark (DTU)
rickr@dtu.dk

Michel Bierlaire
Transport and Mobility Laboratory
Ecole Polytechnique Federale de Lausanne (EPFL)
michel.bierlaire@epfl.ch

April 30, 2024

Abstract

This paper presents an Activity-Based Restriction Model (ABRM) for modeling epidemiological responses during or after a pandemic. The objective of the model is to include pandemic-related restrictions, such as imposed curfews or other activity-restriction policies, when computing activity schedules. Building upon the ABM developed by Pougala *et al.* (2022), this study presents an updated formulation capable of including pandemic restriction and typical responses. In particular, we integrate two key aspects: first, we estimate latent factors that capture the psychological and emotional sensitivity of people to the pandemic's effects, integrating these into the optimization problem. Second, we account for the direct impact of restrictions on activity participation and the adaptive strategies individuals might employ, such as altering the time, location, or nature of their activities. This dual approach allows for a more comprehensive understanding of population behavior in response to public health policies. Moreover, we introduce a dynamic programming algorithm to efficiently solve the updated optimization problem. The use of dynamic programming allows for efficient handling of large-scale populations and numerous activities, a significant advancement over the limitations identified in Pougala *et al.* (2022) using cplex as a solver. This methodological improvement ensures accurate representation of all possible contacts, capturing the true dynamics of infection transmission within the population.

Keywords

Activity-based modeling, agent-based simulation, decision-making, interdisciplinary, and policies.

Contents

List of Tables

List of Figures

1 Introduction

The global COVID-19 pandemic has demonstrated how a disease can deeply disrupt individual daily schedules. On one hand, there are the direct restrictions imposed by governments to contain the spread of the virus, such as lockdowns and curfews. On the other hand, a more subtle but equally significant effect arises as individuals, influenced by their own perceptions of risk, voluntarily adjust their routines and activities. Both government restrictions and personal choices have reshaped daily life patterns, directly influencing how diseases spread. For this reason, it is necessary to understand these changes and introduce them into epidemiological models to study and manage disease transmission more effectively. This paper presents an Activity-Based Model (ABM) developed to simulate and explore the complex interactions between public health policies and individual behaviors during and after pandemics, specifically for the integration with an epidemiological model.

The relationship between human mobility and epidemiology, particularly in the context of COVID-19, has been a focus of significant research. Studies such as those by Hancean *et al.* (2021), Mazzoli *et al.* (2020), and Palguta *et al.* (2022) have explored how human movement patterns influence the transmission dynamics of diseases. Further investigations by Tuomisto *et al.* (2020), Kerr *et al.* (2020), and Aleta *et al.* (2020) have employed detailed mobility data to simulate virus propagation, aiding in the forecasting of outbreak scenarios and the assessment of control measures. Despite these advances, existing models fail to account for how individuals adjust their behaviors in response to health risk perception and restrictions. Furthermore, data privacy policies make the access to real-time GPS tracking data complicate, making it hard to directly capture individuals' actual responses. Indeed, the models proposed by those on the literature (Tuomisto *et al.* (2020), Kerr *et al.* (2020), and Aleta *et al.* (2020)) do not adequately predict changes in activity schedules influenced by personal risk perception. Moreover, they often overlook the potential for activity swapping, such as people frequenting dance classes more often when restaurants are closed, which can significantly alter the dynamics of public space usage and virus transmission. Furthermore, the computational complexity of solving these models increases dramatically with the number of facilities and individuals involved. This rapid escalation in complexity renders the problem quickly intractable, as expanding the scope to realistically represent entire populations interacting with a multitude of facilities demands advanced computational techniques and innovative modeling approaches to remain feasible.

To address these gaps in the literature, our model incorporates a latent model to simulate

individuals' risk perceptions across different activities embedded with an ABM that generates daily schedules of large scale populations taking into account imposed activities restrictions and the the choices of the individuals due to risk perception. The ABM builds on the groundwork established by Pougala *et al.* (2022), expanding its capabilities to include dynamic elements like imposed curfews and other activity-restriction policies. These enhancements are valuable for simulating various public health strategy scenarios, thus supporting policymakers in devising effective, sensitive interventions. Additionally, this paper introduces a sophisticated dynamic programming algorithm that significantly optimizes the activity scheduling problem for large-scale populations. This methodological advance overcomes previous computational challenges, as the problem becomes critically complex as the number of facilities and individuals increases. It is specifically suited for integration with an epidemiological model, effectively linking individual risk perceptions and policy impacts to mobility patterns and disease transmission dynamics.

2 Data

This study uses a detailed survey dataset (see Chauhan *et al.* (2022)) collected during the COVID-19 pandemic to analyze the impacts on individuals' mobility patterns and travel decisions. This dataset allows for the calibration of the latent model which integrates behavioral responses to COVID-19.

The survey dataset includes responses from a diverse demographic, providing detailed information on their mobility patterns, including the frequency of performing activity during the pandemic. Attitudinal variables of the individuals Y_{an} reflect individuals' risk perceptions and concerns regarding the pandemic. These answers are the key in modeling the psychological underpinnings influencing activity-travel behavior during a public health crisis. Each demographic information k of the individual n is represented as x_{kn} in the dataset, as visualized in Appendix B, in Figure 3.

As input for our ABM model, we need to provide a synthetic population that includes individual-level demographic and socio-economic characteristics, as well as a network outlining the spatial layout of activities. In this case, we use the open-source synthetic population provided by He *et al.* (2020), which includes data on individuals' age, gender, employment status, and education level. Additionally, this synthetic dataset integrates a geographic network that assigns coordinates to nodes, each tagged with specific activity types such as leisure, education, shop, work, and home, x_f.

3 Methodology

This section describes the methodology behind our ABRM, which simulates individual responses to public health policies during pandemics. We combine data analysis and simulation to predict changes in mobility and activity based on perceived health risks and regulations.

3.1 Latent Model

Given a dataset containing both attitudinal and explanatory variables, we estimate a latent variable model that captures individuals' perceived risk of COVID-19. The model consists of a structural equation representing the latent construct and a set of measurement equations linking this latent variable to observable indicators.

Structural Equation for the Latent Variable The latent variable for each individual, denoted as X_n^*, represents the high perceived risk and is estimated by the following structural equation:

$$X_n^* = \beta_0^* + \sum_{k=1}^{K} \beta_k^* x_{kn}^* + \sigma\epsilon^* \tag{1}$$

where: i) β_0^* is the intercept, ii) β_k^* are the coefficients for the explanatory variables x_{kn}^* for each individual n, iii) σ is the standard deviation of the error term, iv) ϵ^* represents the error term associated with the latent variable.. The list of the explanatory variables x_{kn}^* can be found in Appendix A, Table 1.

Measurement Equations The indicators, measured on a Likert scale from 1 to 5, indicate the risk perception of performing an activity a by an individual n. This indicators are associated with the latent variable through the following measurement equations:

$$Y_{an}^* = \alpha_{0a}^* + \alpha_a^* X_n^* + \sigma_a^* \xi_a^* \tag{2}$$

where: i) α_{0a}^* is the intercept for the a-th indicator, ii) α_a^* is the coefficient relating the latent variable to the a-th indicator, iii) σ_a^* is the standard deviation of the error term for the a-th indicator, iv) ξ_a^* is the error term for the a-th indicator, v) τ_j are the thresholds

that define the categories of the Likert scale.

$$Y_{an} = \begin{cases} 1 & \text{if } Y_{an}^* < \tau_1, \\ 2 & \text{if } \tau_1 \leq Y_{an}^* < \tau_2, \\ 3 & \text{if } \tau_2 \leq Y_{an}^* < \tau_3, \\ 4 & \text{if } \tau_3 \leq Y_{an}^* < \tau_4, \\ 5 & \text{if } \tau_4 \leq Y_{an}^*. \end{cases} \tag{3}$$

The list of indicators can be found in Appendix A, Table 2. Note that we consider the ones related to risk perception in specific activities. The thresholds τ_j are defined symmetrically around zero to facilitate interpretation. For this reason, we define two positive parameters δ_1^* and δ_2^* as:

$$\begin{aligned} \tau_1 &= -\delta_1^* - \delta_2^*, \\ \tau_2 &= -\delta_1^*, \\ \tau_3 &= \delta_1^*, \\ \tau_4 &= \delta_1^* + \delta_2^*. \end{aligned}$$

Finally, the contribution to the likelihood for the ordered probit model is given by:

$$\begin{aligned} \Pr(Y_{jn} = j_a) &= \Pr(\tau_{j-1} \leq Y_n^* \leq \tau_j) \\ &= \Pr\left(\frac{\tau_{j-1} - \alpha_{0a}^* - \alpha_a^* X_n^*}{\sigma_a^*} < \xi_a \leq \frac{\tau_j - \alpha_{0a}^* - \alpha_a^* X_n^*}{\sigma_a^*} \right) \\ &= \Phi\left(\frac{\tau_j - \alpha_{0a}^* - \alpha_a^* X_n^*}{\sigma_a^*} \right) - \Phi\left(\frac{\tau_{j-1} - \alpha_{0a}^* - \alpha_a^* X_n^*}{\sigma_a^*} \right). \end{aligned}$$

where Φ denotes the cumulative distribution function of the standard normal distribution.

3.2 Activity-Based Mobility Restriction Model

Modeling elements The ABRM operates with three main inputs: individual characteristics, facility characteristics, and imposed policies. The input x_n^e includes characteristics of the individual, such as the personal identifier, city of residence, age, employment status, and home and work identifiers along with their corresponding coordinates. The second input, x_f, details the characteristics of the facilities, where each facility is characterized by its identifier, type (education, shop, or leisure), type identifier, and geographic coordinates in the Swiss projection system. The third input is the Non-Pharmaceutical-Intervention

(NPI), or policy p, where every policy p consists of the activation of the set of parameters belonging to $\mathcal{P}$. Each element of $\mathcal{P}$ is defined as a parameter $\varphi_{\text{restriction},a}$, which takes value 1 if the restriction is activated for activity a, and 0 otherwise. This includes new convex constraints reflecting multiple interventions, such as closure of activities, management of peak hours, travel-time restrictions, curfew restrictions, and outside time limits. Additionally, another critical input of the model are the parameters κ_a and τ_a for all activities, representing the desired starting time and duration of activity a, respectively. To ensure that these simulations reflect realistic and coherent behavior patterns, we derive these parameters from distributions that are calculated based on sub-populations segmented by age and employment status.

Linking the latent with the ABMR Model The integration of the latent model with the ABMR model allows for the capturing on how individual perceptions of pandemic-related risks influence their activity scheduling decisions. The latent model quantifies individual psychological and emotional sensitivities towards various activities through the latent variable X_n^* (Equation (1)). This variable is used to assess risk perception, which is then mapped to a categorical variable (Equations (2) and (3)).

The discretized risk perception categories directly influence the ABMR model by altering the desired duration of activities τ_a for every individual. Specifically, a higher perceived risk associated with an activity leads to a proportional reduction in the time individuals are willing to allocate to that activity. This adaptive behavior is modeled by adjusting the desired activity durations τ_a based on the risk category assigned to an individual, reflecting a realistic modification of daily routines in response to personal risk assessments. For this reason, we define the frequency adjustment coefficient for every individual n and activity a as:

$$\iota_{an} = 1 - \frac{\text{Frequency of } a \text{ per week for individual } n}{\text{Max frequency observed for any activity}}, \tag{4}$$

and the new desired duration τ_a' becomes:

$$\tau_a' = \tau_a(1 + (Y_{an} - 1)\iota_{an}). \tag{5}$$

Note that the frequencies of each activity per week an individual are observed in Chauhan *et al.* (2022). Through this mechanism, the ABMR model dynamically incorporates individual-level responses into the simulation of mobility and activity patterns.

Optimization problem definition The foundational structure of the utility function is adapted from Pougala *et al.* (2022). This work builds upon the existing framework by intro-

ducing additional terms in the objective function, including the latent class for high-risk perception, and incorporating new constraints to address the mobility restrictions. We define the set of restrictions as $\mathcal{P}$ where each element is defined as $\varphi_{\text{restriction},a}$, $\forall$ restriction $\in \mathcal{R}$, where restrictions is a vector where each element corresponds to a specific type of restriction as restrictions$_i$ = $\{1$: closure restrictions, 2 : time slot starting time restrictions, 3 : time slot closing time restrictions, 4 : peak hour restrictions, 5 : travel time restrictions, 6 : curfew restrictions$\}$, where i is the index of the vector element. Given a set of activities $\mathcal{A}$, and a set of restrictions $\mathcal{P}$, the optimization problem can be defined as:

$$\max_{\omega,Z,x,\tau} \quad U_0 + \sum_{a=0}^{A} Z_a^0(\chi_a + V_a^1 + V_a^2 + \varphi_{5,a}V_{ab}^3) + \sum_{a=0}^{A}\sum_{b=0}^{A} Z_{ab} \cdot \theta_t \cdot \omega_{ab} \tag{6}$$

subject to:

$$\sum_a \sum_b (Z_a^0 \cdot x_a^2 + Z_{ab} \cdot \omega_{ab}) = 24 \tag{7}$$

$$\omega_{\text{dawn}} = \omega_{\text{dusk}} = 1 \tag{8}$$

$$x_a^2 \geq Z_a^0 \cdot \tau_a^{\min} \qquad \forall a \in \mathcal{A} \tag{9}$$

$$x_a^2 \leq Z_a^0 \cdot T \qquad \forall a \in \mathcal{A} \tag{10}$$

$$Z_{ab} + Z_{ba} \leq 1 \qquad \forall a, b \in \mathcal{A}, a \neq b \tag{11}$$

$$Z_{a,\text{dawn}} = Z_{\text{dusk},a} = 0 \qquad \forall a \in \mathcal{A} \tag{12}$$

$$\sum_a Z_{ab} = Z_b^0 \qquad \forall b \in \mathcal{A}, b \neq \text{dawn} \tag{13}$$

$$\sum_b Z_{ab} = Z_a^0 \qquad \forall a \in \mathcal{A}, a \neq \text{dusk} \tag{14}$$

$$(Z_{ab} - 1) \cdot T \leq x_a^1 + x_a^2 + Z_{ab} \cdot \omega_{ab} - x_b^1 \qquad \forall a, b \in \mathcal{A}, a \neq b, \tag{15}$$

$$(1 - Z_{ab}) \cdot T \geq x_a^1 + x_a^2 + Z_{ab} \cdot \omega_{ab} - x_b^1 \qquad \forall a, b \in \mathcal{A}, a \neq b \tag{16}$$

$$x_a^1 \geq \chi_a^- \qquad \forall a \in \mathcal{A} \tag{17}$$

$$x_a^1 + x_a^2 \leq \chi_a^+ \qquad \forall a \in \mathcal{A} \tag{18}$$

$$\sum_{a \in \mathcal{F}_a} Z_a^0 \leq 1 \qquad \forall a \in \mathcal{A} \tag{19}$$

$$\varphi_{1,a} Z_a^0 = 0 \qquad \forall \varphi_{1,a} \in \mathcal{P}, a \in \mathcal{A} \tag{20}$$

$$\varphi_{2,a} x_a^1 \geq \varphi_{2,a} t_\Theta^1 \qquad \forall \varphi_{2,a} \in \mathcal{P}, a \in \mathcal{A} \tag{21}$$

$$\varphi_{3,a}(x_a^1 + x_a^2) \geq \varphi_{3,a} t_\Theta^2 \qquad \forall \varphi_{3,a} \in \mathcal{P}, a \in \mathcal{A} \tag{22}$$

$$\varphi_{4,a}(x_a^1 + x_a^2) \leq \varphi_{4,a}(t_\Theta^3 + 24 * (1 - Z_2)) \qquad \forall \varphi_{4,a} \in \mathcal{P}, a \in \mathcal{A} \tag{23}$$

$$\varphi_{4,a} x_a^1 \geq \varphi_{4,a}(t_\Theta^4 - 24 * (1 - Z_1)) \qquad \forall \varphi_{4,a} \in \mathcal{P}, a \in \mathcal{A} \tag{24}$$

$$\varphi_{4,a}(Z_1 + Z_2 - 1) \geq 0 \qquad \forall a \in \mathcal{A} \tag{25}$$

$$\varphi_{5,a}(Z_{ab} \cdot \omega_{ab}) \leq \varphi_{5,a} t_{\Theta}^{5} \qquad \forall \varphi_{5,a} \in \mathcal{P}, a \in \mathcal{A} \tag{26}$$

$$\varphi_{6,a} \tau_{\text{dawn}} \leq \varphi_{6,a} t_{\Theta}^{6} \qquad \forall a \in \mathcal{A} \tag{27}$$

$$\varphi_{6,a} x_{\text{dusk}} \geq \varphi_{6,a} t_{\Theta}^{7} \qquad \forall a \in \mathcal{A} \tag{28}$$

where:

$$V_a^1 = \theta_a^{\text{early}} \cdot \max(0, \kappa_a - x_a^1 - \Delta_a^{\text{early}}) + \theta_a^{\text{late}} \cdot \max(0, x_a^1 - \kappa_a - \Delta_a^{\text{late}}) \tag{29}$$

$$V_a^2 = \theta_a^{\text{short}} \cdot \max(0, \tau_a - x_a^2 - \Delta_a^{\text{short}}) + \theta_a^{\text{long}} \cdot \max(0, x_a^2 - \tau_a - \Delta_a^{\text{long}}) \tag{30}$$

$$V_{ab}^3 = \theta_t \cdot \omega_{ab} \tag{31}$$

Note that restrictions from (7)–(19) are directly taken from Pougala *et al.* (2022). To efficiently handle problem (6)–(28), we employ a dynamic programming approach. A detailed explanation of the latter is provided in Appendix C.

4 Results

To analyze the effectiveness of our model and ensure that the outputs are logical and accurate, we conduct simulations for a sample of 1,000 individuals, and 1236 facilities. We explore seven different scenarios, each representing a different imposed NPI, as detailed by Table 3 in Appendix A. These results show the model's computational robustness.

4.1 Validation of the results in an aggregated and disaggregated way

Aggregated Validation of Activity Patterns Throughout Scenarios In the aggregated analysis, we check for the total number of individuals engaged in each activity type across different intervention scenarios throughout the day. Figure 1 allows us to assess whether the simulated activity patterns align with the restrictions we have imposed. The 'Normal Life' scenario (Subfigure 1(a)) provides a baseline for comparison, depicting a typical day without restrictions. In the 'Outings Limitation' scenario (Subfigure 1(b)), we observe a reduction in non-essential activities, while the 'Early Curfew' scenario (Subfigure 1(c)) reveals a significant decline in evening activities, reflecting adherence to the curfew. Finally, the 'Secondary Facilities Closure' scenario (Subfigure 1(d)) shows the closing of secondary activities, corresponding to the targeted policy action. The changes across these scenarios align with the constraints imposed in our simulation, providing initial validation that the model behaves as expected. These aggregated results demonstrate coherent and realistic adjustments in the population's activity patterns in response to the different NPIs.

Figure 1: Aggregated visualization of total count of individuals' in each activity throughout the day under various scenarios.

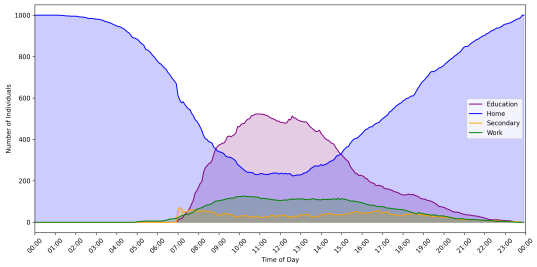

(a) Normal life

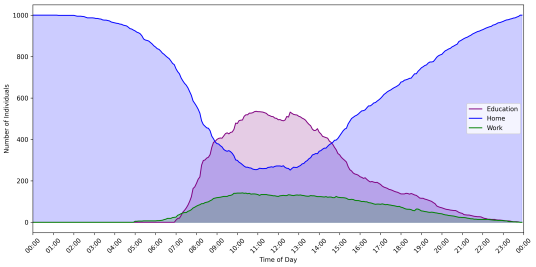

(b) Outings limitation

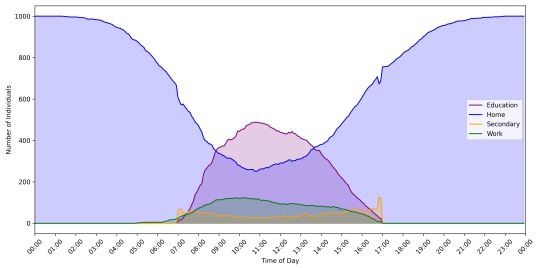

(c) Early curfew

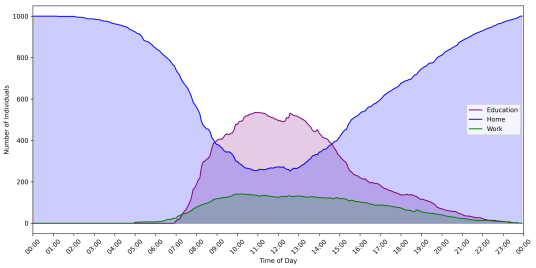

(d) Impact of secondary facilities closure

Disaggregated Validation of the Baseline Scenario To further validate the model, we examine the schedules of different individuals in the baseline scenario, ensuring that the simulation captures the variability inherent in real-world behavior. Figures 2(a), 2(b), and 2(c), each display the typical daily schedules for a student child, working adult, and university student, respectively. These schedules show that the model accurately reflects individual variations in activity patterns, which is critical for the realistic simulation of disease spread. The ability of the model to capture such detail at the individual level underscores its robustness and suitability for further epidemiological analysis.

5 Conclusions

This study has successfully developed an Activity-Based Model (ABM) that integrates individual risk perceptions with mobility patterns under different Non-Pharmaceutical Interventions (NPIs). The model demonstrates a high level of computational robustness, efficiently managing a large-scale simulation of activity patterns across various public health scenarios. Our results indicate that the model operates coherently, producing both aggregated and disaggregated activity schedules that are realistic and sensible under imposed conditions. However, the model's current validation is based on a limited sample size and scenario range. Future work will extend this

Figure 2: Individual daily schedules in the baseline scenario validate the model's ability to simulate realistic and diverse activity patterns.

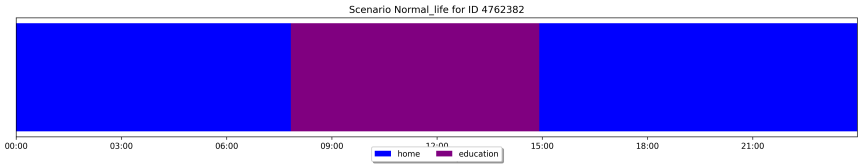

(a) Daily schedule of a student child, reflecting a balance between education and time spent at home.

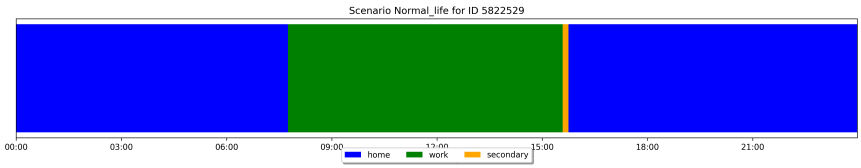

(b) Daily schedule of a working adult, showing a clear division between work hours and time at home.

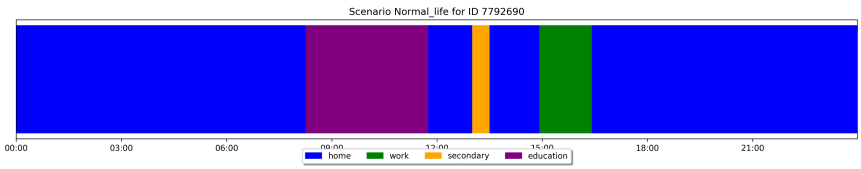

(c) Daily schedule of a university student, indicating a mixture of educational activities and personal time.

to a larger population sample, although this expansion introduces computational complexities due to the increased number of interactions and the detailed level of data required. Additionally, integrating the latent model for risk perception more deeply will allow us to refine the simulation of activity durations based on individual behavioral responses to perceived risks. To further validate our model, we aim to align our simulation outputs with mobility data from sources like Google, which will provide empirical insights into how restrictions and risk perceptions actually impact mobility patterns. This step is critical for enhancing the model's accuracy and applicability in real-world scenarios. Ultimately, by embedding this refined model within the epidemiological framework proposed by Cortes Balcells *et al.* (2023), we can simulate and evaluate the effectiveness of various public health policies. This will enable policymakers to design interventions that are not only effective but also adaptive to the public's behavioral responses, optimizing health outcomes in future pandemics.

6 References

Aleta, A., D. Martin-Corral, A. Pastore Y Piontti, M. Ajelli, M. Litvinova, M. Chinazzi, N. E. Dean, M. E. Halloran, I. M. Longini, S. Merler, A. Pentland, A. Vespignani, E. Moro and Y. Moreno (2020) Modelling the impact of testing, contact tracing and household quarantine on second waves of COVID-19, *Nature Human Behaviour*, **4** (9) 964–971, ISSN 2397-3374.

Chauhan, R. S., M. W. Bhagat-Conway, T. Magassy, N. Corcoran, E. Rahimi, A. Dirks, R. Pendyala, A. Mohammadian, S. Derrible and D. Salon (2022) COVID Future Panel Survey: A Unique Public Dataset Documenting How U.S. Residents' Travel Related Choices Changed During the COVID-19 Pandemic, `http://arxiv.org/abs/2208.12618`. ArXiv:2208.12618 [cs, stat].

Cortes Balcells, C., R. Krueger and M. Bierlaire (2023) Multi-objective Optimization of Activity-Travel Policies for Epidemic Control: Balancing Health and Economic Outcomes on Socio-Economic Segments.

Hancean, M.-G., M. Slavinec and M. Perc (2021) The impact of human mobility networks on the global spread of COVID-19, *Journal of Complex Networks*, **8** (6) cnaa041, ISSN 2051-1310, 2051-1329.

He, B. Y., J. Zhou, Z. Ma, J. Y. Chow and K. Ozbay (2020) Evaluation of city-scale built environment policies in New York City with an emerging-mobility-accessible synthetic population, *Transportation Research Part A: Policy and Practice*, **141**, 444–467, ISSN 09658564.

Kerr, C. C., R. M. Stuart, D. Mistry, R. G. Abeysuriya, G. Hart, K. Rosenfeld, P. Selvaraj, R. C. Nunez, B. Hagedorn, L. George, A. Izzo, A. Palmer, D. Delport, C. Bennette, B. Wagner, S. Chang, J. A. Cohen, J. Panovska Griffiths, M. Jastrzebski, A. P. Oron, E. Wenger, M. Famulare and D. J. Klein (2020) Covasim: an agent-based model of COVID-19 dynamics and interventions, `https://www.medrxiv.org/content/10.1101/2020.05.10.20097469v1`. Pages: 2020.05.10.20097469.

Mazzoli, M., D. Mateo, A. Hernando, S. Meloni and J. J. Ramasco (2020) Effects of mobility and multi-seeding on the propagation of the COVID-19 in Spain, *preprint*, Epidemiology.

Palguta, J., R. Levinsky and S. Skoda (2022) Do elections accelerate the COVID-19 pandemic?: Evidence from a natural experiment, *Journal of Population Economics*, **35** (1) 197–240, ISSN 0933-1433, 1432-1475.

Pougala, J., T. Hillel and M. Bierlaire (2022) Capturing trade-offs between daily scheduling choices, *Journal of Choice Modelling*, **43**, 100354, ISSN 17555345.

Torres, F., M. Gendreau and W. Rei (2022a) Crowdshipping: An open VRP variant with stochastic destinations, *Transportation Research Part C: Emerging Technologies*, **140**, 103677. Publisher: Elsevier.

Torres, F., M. Gendreau and W. Rei (2022b) Vehicle Routing with Stochastic Supply of Crowd Vehicles and Time Windows, *Transportation Science*, **56** (3) 631–653, ISSN 0041-1655, 1526-5447.

Tuomisto, J. T., J. Yrjola, M. Kolehmainen, J. Bonsdorff, J. Pekkanen and T. Tikkanen (2020) An agent-based epidemic model REINA for COVID-19 to identify destructive policies, *preprint*, Infectious Diseases (except HIV/AIDS).

A Tables

Table 1: Explanatory variables for the Latent Model

Variable Name	**Description**	**Type**
age_above_60	Is the individual above 60 years old?	Binary
age_bw_30_60	Is the individual between 30 and 60 years old?	Binary
age_under_30	Is the individual under 30 years old?	Binary
gender_female	Is the individual female?	Binary
notCaucasian	Is the individual not Caucasian?	Binary
bachelors_or_more	Does the individual have a bachelor's degree or more?	Binary
technical_school	Did the individual attend technical school?	Binary
high_school	Did the individual graduate from high school?	Binary
worker	Is the individual currently employed?	Binary
zone_Midwest	Is the individual located in the Midwest zone?	Binary
zone_Northeast	Is the individual located in the Northeast zone?	Binary
zone_South	Is the individual located in the South zone?	Binary
zone_West	Is the individual located in the West zone?	Binary
income_below_35	Is the individual's income below $35,000?	Binary
income_35_to_100	Is the individual's income between $35,000 and $100,000?	Binary
income_above_100	Is the individual's income above $100,000?	Binary
hh_single	Is the household single?	Binary
hh_partner	Is the household in partnership?	Binary
hh_children	Does the household have children?	Binary
hh_parents	Does the household have parents?	Binary
single_only	Is the individual single only in the household?	Binary
partner_only	Is the individual in partnership only in the household?	Binary
children_only	Is the individual responsible for children only in the household?	Binary
parents_only	Is the individual responsible for parents only in the household?	Binary
partner_and_children	Is the individual in partnership and responsible for children in the household?	Binary
partner_and_parents	Is the individual in partnership and responsible for parents in the household?	Binary
children_and_parents	Is the individual responsible for both children and parents in the household?	Binary
multiple_automobiles	Does the household own multiple automobiles?	Binary
hhsize_1	Is the household size 1?	Binary
hhsize_2	Is the household size 2?	Binary
hhsize_3	Is the household size 3?	Binary
hhsize_4	Is the household size 4?	Binary
hhsize_4plus	Is the household size more than 4?	Binary
hhfamilyhouse	Is the household a family house?	Binary
hhapartment	Is the household an apartment?	Binary
covid_positive	Is the individual COVID-19 positive?	Binary

Table 2: COVID-19 Attitudes and Risk Perception Indicators. Coding for agreeing indicators: 1=Strongly disagree, 2=Somewhat disagree,3=Neutral, 4=Somewhat agree, 5=Strongly agree, -1= Question not displayed to respondent. Coding for risk indicators:1=Extremely low risk, 2= Low risk, 3=Medium risk, 4=High risk, 5=Extremely high risk.

Indicator Name	**Description**
att_covid_1	If I catch the coronavirus, I am concerned that I will have a severe reaction.
att_covid_2	I am concerned that friends or family members will have a severe reaction to the coronavirus if they catch it.
att_covid_3	Everyone should just stay home as much as possible until the coronavirus has subsided.
att_covid_4	Society is overreacting to the coronavirus.
att_covid_5	Shutting down businesses to prevent the spread of coronavirus is not worth the economic damage that will result.
att_covid_6	My friends and family expect me to stay at home until the coronavirus subsides.
att_covid_7	Everyone should wear a mask when in public indoor spaces.
att_covid_8	The COVID-19 vaccines available in the U.S. are safe.
att_covid_9	Getting vaccinated will protect me from COVID-19.
risk_percp_1	How do you perceive your COVID-19 risk from going to work?
risk_percp_2	How do you perceive your COVID-19 risk from shopping at a grocery store?
risk_percp_3	How do you perceive your COVID-19 risk from riding public transportation?
risk_percp_4	How do you perceive your COVID-19 risk from walking or bicycling?
risk_percp_5	How do you perceive your COVID-19 risk from taking a taxi or ride-hailing service?
risk_percp_6	How do you perceive your COVID-19 risk from traveling in an airplane?
risk_percp_7	How do you perceive your COVID-19 risk from sending children to school?

Table 3: Tested scenarios, each one considering different NPIs as input to the ABM.

Tested Scenarios	**Closure**			**Constraints**
	Leisure	**Education**	**Work**	**Curfew**
No restrictions				
Outing limitations	x			
Early curfew				5pm
Economy preservation	x	x		
Work-education balance		x	x	
Leisure facilities closure	x			

B Figures

Figure 3 includes histograms that illustrate the distribution of respondents' characteristics. The top-left histogram displays the age distribution, indicating a wide range of participant ages with a concentration in the middle-age individuals. The top-right histogram categorizes respondents

Figure 3: Demographic distribution of survey respondents.

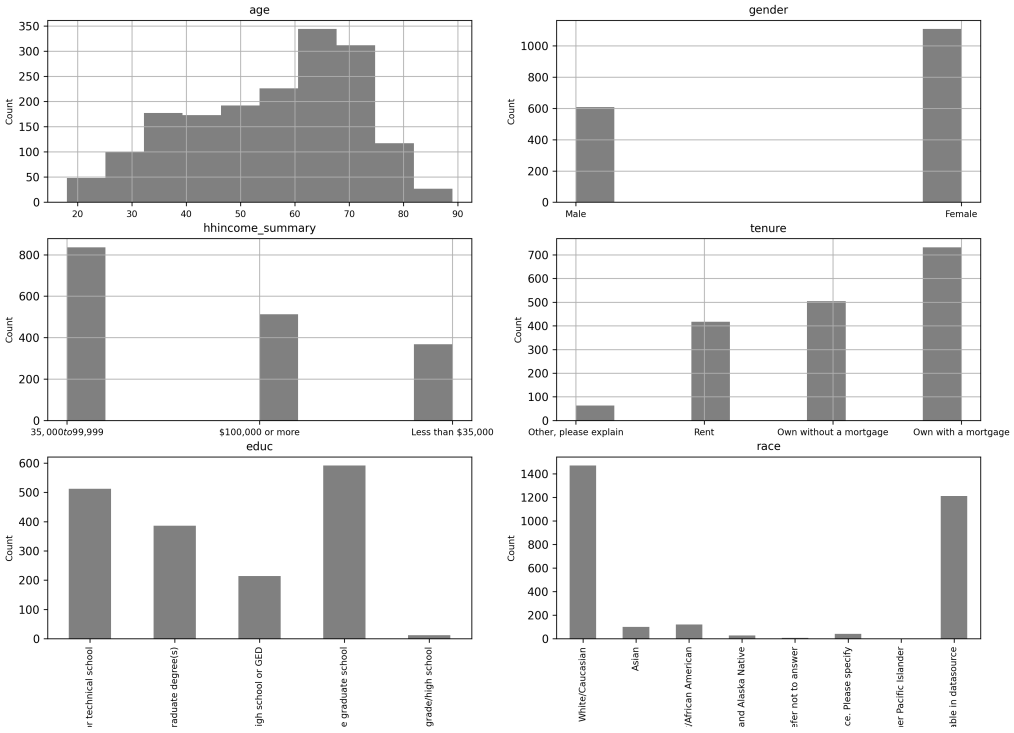

by gender, showing a higher count of female participants compared to male. The middle-left histogram provides a summary of household income, with the majority of respondents reporting an income of less than $35,000$ or between $35,000$ and $99,999$. Education levels, plotted in the middle-right histogram, reveal that most participants have completed some college or obtained a bachelor's degree. The bottom-left histogram depicts housing tenure, with the predominant categories being 'Own with a mortgage' and 'Rent.' Finally, the bottom-right histogram classifies respondents by race, with a notably higher representation of White/Caucasian individuals.

C Computational Complexity and Dynamic programming algorithm

Since the goal of the ABM is to be included in an epidemiological activity-based model, the facility choice set needs to match the population size. This need arises from the fact a limited number of facilities can result in overcrowding, thereby escalating the virus transmission, whereas an excessively large number of facilities can spread out the gatherings, consequently reducing the virus spread. The problem with increasing the number of facilities is that the execution time is affected by the choice set size, growing exponentially with more options. In fact, solving model (6)-(28) with commercial solvers is slow and the model is intractable even for small instances with a few activities. To address this problem, we make the assumption that an individual only considers the closest facilities to them. This assumption is restrictive but does not impact the ABM results, since there is no benefit in traveling further to do an activity that could have been done closer. The number of nearby facilities to work and home is user-defined. In addition, we use an advanced dynamic programming algorithm to solve the problem, by representing model (6)-(28) in a network allowing us to reduce computation complexity, as discussed in the following paragraph.

The problem can be described as an elementary shortest path problem with resource constraints which is a common sub-problem for the solution of vehicle routing problems. The method used to solve this variant of the shortest path problem is usually a dynamic programming method, also known as labeling algorithms (e.g., Torres *et al.* (2022a,b)). To describe the Dynamic Programming algorithm, we first discretize the time into 288 intervals for every 5 minutes. We define a state using a label $\mathcal{L} = (a, U, t, x_a^3, u, \mathcal{R})$, where a is the current activity, U is the total utility collected including the current activity, t is the time interval, x_a^3 is the duration of the activity, u is the cumulative cost, and $\mathcal{R}$ is the set of activities that cannot be reached either because they have been completed or are mutually exclusive with completed activities.

The algorithm starts with an initial label that represents the start of the day. In each iteration, it explores all possible activities, creating new labels with updated states. Resources are extended through resource extension functions which keep track and update resource consumption. To extend a label $\mathcal{L}_k$ to a new activity a_j, we first check if the extension is feasible, ensuring that no constraints (such as time or budget) are violated and a_j is not in $\mathscr{U}_j$. If feasible, we create a new label $\mathcal{L}_j$ with updated resource states.